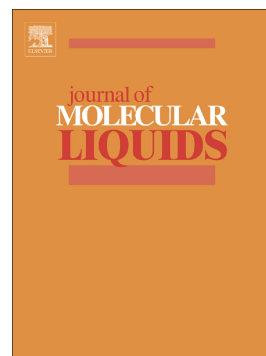


Accepted Manuscript

Tacrine-pyrimidine photoactive molecular hybrids: Synthesis, photophysics, docking and BSA interaction study

João Paulo Bizarro Lopes, Viktor Saraiva Câmara, Dennis Russowsky, Pablo Andrei Nogara, João Batista Teixeira da Rocha, Fabiano da Silveira Santos, Fabiano Severo Rodembusch, Marco Antonio Ceschi



PII: S0167-7322(19)31802-1
DOI: <https://doi.org/10.1016/j.molliq.2019.110983>
Article Number: 110983
Reference: MOLLIQ 110983
To appear in: *Journal of Molecular Liquids*
Received date: 28 March 2019
Revised date: 7 May 2019
Accepted date: 15 May 2019

Please cite this article as: J.P.B. Lopes, V.S. Câmara, D. Russowsky, et al., Tacrine-pyrimidine photoactive molecular hybrids: Synthesis, photophysics, docking and BSA interaction study, *Journal of Molecular Liquids*, <https://doi.org/10.1016/j.molliq.2019.110983>

This is a PDF file of an unedited manuscript that has been accepted for publication. As a service to our customers we are providing this early version of the manuscript. The manuscript will undergo copyediting, typesetting, and review of the resulting proof before it is published in its final form. Please note that during the production process errors may be discovered which could affect the content, and all legal disclaimers that apply to the journal pertain.

Tacrine-pyrimidine photoactive molecular hybrids: synthesis, photophysics, docking and BSA interaction study

João Paulo Bizarro Lopes,^{a,*} Viktor Saraiva Câmara,^a Dennis Russowsky,^b Pablo Andrei Nogara,^c João Batista Teixeira da Rocha,^c Fabiano da Silveira Santos,^d Fabiano Severo Rodembusch,^{d,*} Marco Antonio Ceschi^a

^aInstituto de Química, Universidade Federal do Rio Grande do Sul, Av. Bento Gonçalves, 9500, Campus do Vale, 91501-970, Porto Alegre, RS, Brazil. E-mail: joaopauloblopes@terra.com.br

^bLaboratório de Sínteses Orgânicas K210, Instituto de Química, Universidade Federal do Rio Grande do Sul, Av. Bento Gonçalves 9500, Porto Alegre, Rio Grande do Sul, Brazil.

^cDepartamento de Bioquímica e Biologia Molecular, Centro de Ciências Naturais e Exatas, Universidade Federal de Santa Maria - UFSM, RS, Brazil

^dGrupo de Pesquisa em Fotoquímica Orgânica Aplicada, Instituto de Química, Universidade Federal do Rio Grande do Sul, Av. Bento Gonçalves 9500, Porto Alegre, Rio Grande do Sul, Brazil. E-mail: rodembusch@iq.ufrgs.br

Abstract

This study reports the synthesis of two photoactive molecular hybrids containing Tacrine and pyrimidine moieties achieved by multicomponent reaction. The hybrids **11a** and **11b** present absorption maxima close to the Tacrine absorption (~320 nm). The hybrids present fluorescence emission around 400 nm, as observed for the separate Tacrine and pyrimidine structures. Time-resolved fluorescence indicates for **11a** and **11b** a monoexponential time decay around 1.5 ns. In this sense, the variation on the size of the aliphatic linker between both fluorophores seems not to affect the observed photophysical properties of the hybrids. In addition, the interaction of the compounds with bovine serum albumin (BSA) in phosphate buffer solution (PBS) was investigated, where a suppression mechanism was observed for both molecular hybrids. Docking was also performed to better understand the observed suppression mechanism.

1. Introduction

The use of fluorescent molecular probes has enabled to understand the functioning of the human body at a molecular level and to monitor biochemical processes of specific interactions [1]. Exhibiting a high level of sensitivity, fluorescence has emerged as a substitute for radioactivity on the generation of images from biological materials [2,3]. Different small fluorescent compounds have been developed for medical diagnostic imaging such as fluorescein and rhodamine [4]. Recently, a study in patients showed that the fluorescence of acridine orange, a quinoline derivative dye, can be used on a staining method for screening of circulating tumour cells [5].

Quinoline is known as a fluorophore unit which is present in small molecular fluorescent compounds such as acridine orange (Figure 1) [6]. Quinoline derivatives are also well known for their good metal affinity and are emerging from fluorescent probes for zinc and their applications in more complex biological research [7]. Recently, Wang *et al.* synthesized acridine-based fluorescence chemosensors with selective sensitivity for Fe^{3+} and Ni^{2+} ions [8]. Tacrine is an important quinoline structural derivative which was the first drug approved by the FDA, in 1993, for the treatment of Alzheimer's disease (AD). Although its use has been discontinued for a decade, Tacrine still have boosted the search of novel therapeutic compounds for AD [9,10,11,12,13]. On the other hand, dihydropyrimidin-2-ones (DHPMs, Figure 1), known as Biginelli adducts, are heterocyclic compounds with a broad spectrum of biological activity, such as antibacterial, anti-inflammatory, antiviral and specially anticancer [14]. DHPMs have been reported to exhibit fluorescence and photophysical properties, making them potential candidates for molecular probes [15,16]. Recently, we synthesized two lophine-pyrimidine hybrids which exhibit fluorescence properties that probably experience photoinduced electron transfer (PET) in the excited state. Also, they presented BSA suppression probably due to the pyrimidine moiety, which presented a higher Stern-Volmer constant in comparison to lophine [17].

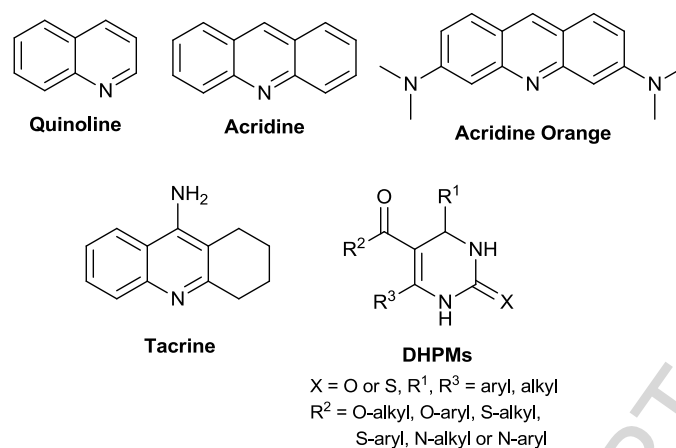


Figure 1. Quinoline derivatives and Biginelli adducts DHPMs.

Bovine serum albumin (BSA) is often selected as a model of drug-albumin interaction due to its low cost, ready availability and the homology with human serum albumins (HSA) [18,19]. Serum albumins are carrier proteins soluble in plasma that play an essential role in the transport and disposition of endogenous and exogenous compounds in blood, such as metabolites, drugs and other organic compounds [20]. The study of the drug–albumin interaction contributes to information on the absorption, transportation, metabolism, distribution and efficacy of drugs in the body [21]. The potential application of fluorescence spectroscopy to study the binding of small molecules to serum albumins have been widely recognized for allowing non-intrusive measurements of substances under physiological conditions [22]. In 2011, Chen and co-workers showed that intrinsic fluorescence of HSA was quenched by 9-aminoacridine derivatives [21]. Also, some studies have demonstrated that acridine orange dye can interact with BSA quenching their fluorescence and increase the degree of damage to protein molecules [20,23].

In this study, it was synthesized novel hybrids containing both Tacrine and pyrimidine from the Biginelli DHPM moiety, connected by a methylene chain as an aliphatic linker. The two novel Tacrine-pyrimidine hybrids were evaluated by UV-Vis and fluorescence emission in order to improve the understanding of their photophysical properties. Their potential application as fluorescent probes to detect proteins in phosphate buffer solution (PBS) was also explored using BSA as a model. Also, molecular modelling studies were performed to understand the binding mode of ligand in the BSA.

2. Experimental

2.1. Materials and methods

Purification of products by column chromatography was carried out on silica gel 60 Å (70-230 mesh). Analytical thin layer chromatography (TLC) was conducted on aluminium plates with 0.2 mm of silica gel 60F-254 (Macherey-Nagel). Solvents were obtained from Tedia and Nuclear, and reagents were purchased from Sigma-Aldrich, Acros Organics and TCI. The following compounds were preparing according to previous literature protocol: **3** [24], amines **5a** and **5b** [25], DHPM **9** and pyrimidine **10** [26,27,28]. All infrared spectra were recorded on a Varian 640-IR spectrometer in KBr disks. ¹H NMR and ¹³C NMR spectra were recorded in CDCl₃ solution on a Varian VNMRs 300 MHz spectrometer. The assignment of chemical shifts is based on standard NMR experiments (¹H; ¹³C; ¹H, ¹H-COSY; ¹H, ¹³C-HMQC). Chemical shifts (δ are in part per million from the peak of tetramethylsilane ($\delta = 0.00$ ppm as internal standard in ¹H NMR or from the solvent peak of CDCl₃ ($\delta = 77.23$ ppm in ¹³C NMR); and multiplicities are given as s (singlet), d (doublet), dd (double doublet), t (triplet), q (quartet), m (multiplet) or br (broad); coupling constants (*J*) are given in Hz. High Resolution Mass Spectrometry with Eletrospray Ionisation (HRMS-ESI) data on the positive mode was collected on a UHPLC-QTOF/MS Bruker Impact II instrument. The instrument settings were the following: capillary voltage 4500 V, End Plate Offset Voltage 500 V, dry gas temperature 200 °C. Nitrogen was used as the desolvation gas. Methanol (Tedia HPLC grade) was used as solvent for the analyzed samples and filtered prior to injection.

2.2. General procedure for the preparation of hybrids **11a** and **11b**

A mixture containing the ethyl 2-chloro-4-methyl-6-phenylpyrimidine-5-carboxylate (**10**) (0.6 mmol) and *N*¹-(1,2,3,4-tetrahydroacridin-9-yl)hexane-1,6-diamine (**5a**) or *N*¹-(1,2,3,4-tetrahydroacridin-9-yl)octane-1,8-diamine (**5b**) (0.4 mmol) was diluted in *n*-pentanol (2.0 mL) and refluxed during 48h. After this time, the solvent was removed under vacuum at 120 °C for an hour and the mixture was diluted in CH₂Cl₂ (10 mL). The organic layer was washed with 10 mL of aqueous solutions of NaOH (10%) and brine, dried (Na₂SO₄) and concentrated under vacuum. The crude oil was purified by column

chromatography (eluting with hexane- ethyl acetate- triethylamine, 95:4:1 until 80:19:1) to give the desired product.

2.2.1. Ethyl 4-methyl-6-phenyl-2-((6-((1,2,3,4-tetrahydroacridin-9-yl)amino)hexyl)amino)pyrimidine-5-carboxylate (**11a**). Intermediate **10** and amine **5a** were reacted according to general procedure to give the desired product as a yellow oil (75% yield). IR (*KBr*) ν_{max}/cm^{-1} : 3389, 3261, 2926, 2850, 1710, 1556, 1253, 1074, 754, 692; ^1H NMR (CDCl_3 , 300 MHz) δ 7.99-7.87 (m, 2H), 7.55 (ddd, $J = 8.3, 6.8$ and 1.3 Hz, 3H), 7.44-7.36 (m, 3H), 7.34 (ddd, $J = 8.3, 6.8$ and 1.3 Hz, 1H), 5.31 (t, $J = 5.7$ Hz, 1H), 4.05 (q, $J = 7.1$ Hz, 2H), 3.54-3.36 (m, 4H), 3.12-2.98 (m, 2H), 2.75-2.61 (m, 2H), 2.49 (s, 3H), 1.97-1.83 (m, 4H), 1.72-1.51 (m, 4H), 1.49-1.33 (m, 4H), 0.94 (t, $J = 7.1$ Hz, 3H); ^{13}C NMR (CDCl_3 , 75 MHz) δ 169.0, 166.2, 161.3, 158.3, 151.0, 147.3, 139.3, 129.5, 128.5, 128.5, 128.3, 128.0, 123.7, 123.0, 120.2, 115.8, 115.2, 61.2, 49.5, 41.2, 33.9, 31.8, 29.6, 26.8, 26.7, 24.9, 23.1, 22.8, 13.7; HRMS-ESI: calcd for $[\text{M-H}]^+$ 538.3177, found 538.3186.

2.2.2. Ethyl 4-methyl-6-phenyl-2-((8-((1,2,3,4-tetrahydroacridin-9-yl)amino)octyl)amino)pyrimidine-5-carboxylate (**11b**). Intermediate **10** and amine **5b** were reacted according to general procedure to give the desired product as a yellow oil (67% yield). IR (*KBr*) ν_{max}/cm^{-1} : 3389, 3262, 2922, 2850, 1712, 1562, 1255, 1074, 756, 692; ^1H NMR (CDCl_3 , 300 MHz) δ 7.93 (dd, $J = 15.2$ and 8.5 Hz, 2H), 7.59-7.49 (m, 3H), 7.43-7.36 (m, 3H), 7.36-7.30 (m, 1H), 5.47 (s, 1H), 4.12-3.97 (m, 2H), 3.54 – 3.37 (m, 4H), 3.05 (s, 2H), 2.69 (s, 2H), 2.48 (s, 3H), 1.90 (d, $J = 2.9$ Hz, 4H), 1.70-1.50 (m, 4H), 1.32 (s, 8H), 0.94 (t, $J = 7.1$ Hz, 3H); ^{13}C NMR (CDCl_3 , 75 MHz) δ 169.0, 166.3, 161.4, 158.3, 151.1, 147.3, 139.4, 129.5, 128.5, 128.3, 128.1, 123.8, 123.0, 120.2, 115.8, 115.2, 61.1, 49.6, 41.4, 33.9, 31.9, 29.7, 29.4, 29.3, 27.0, 26.9, 24.9, 23.1, 22.8, 13.7; HRMS-ESI: calcd for $[\text{M-H}]^+$ 566.3490, found 566.3491.

2.3. Photophysical Studies

UV-Vis absorption spectra in solution were performed on a Shimadzu UV-2450 spectrophotometer at a concentration of 10^{-5} M. Steady state fluorescence

spectra were taken using a Shimadzu spectrofluorometer model RF-5301PC. The maximum absorption wavelength was used as the excitation radiation for emission spectra. Slits of 5.0 nm/5.0 nm were used for emission/excitation, respectively. The quantum yields of fluorescence (Φ_{FL}) were measured at 25°C using solutions with absorbance intensity lower than 0.05 (optical dilute regime). In these experiments the emission spectra was obtained using slits of 1.5 nm/1.5 nm (Exc/Em). Quinine sulfate ($\lambda_{exc}=320$ nm) in H₂SO₄ 1N and naphthalene in cyclohexane ($\lambda_{exc}=270$ nm) was used as the quantum yield standards [29,30]. Fluorescence time decay curves were performed in 1,4-dioxane and acetonitrile with an EasyLife V spectrophotometer (OBB). All measurements were performed at room temperature (25 °C). The fluorescence decay curves were analysed using the software EasyLife V from OBB. A nonlinear least square method was employed for the fit of the decay to a sum of exponentials. The value of χ^2 , residuals and the autocorrelation function were used to determine the quality of the fit.

2.4. BSA interaction studies

The BSA association study was performed keeping the dye concentration constant (2 μ M in PBS). In this study different amounts of a previously prepared BSA solutions (0-12 μ M in PBS, pH 7.2) were added. The final solution was kept to rest for 1h. The fluorescence spectra were obtained at 25°C and under excitation at 320 nm (**11a** and **11b**), 345 nm (**1**) and 277 nm (**7**) using Exc/Em slits of 5.0 nm/5.0 nm, respectively. The BSA suppression study was performed keeping the BSA concentration constant (11 μ M in PBS, pH 7.2) and amounts of a previously prepared dye solutions (0-20 μ M in DMSO) were added. The fluorescence spectra were obtained at 25 °C and under excitation at 277 nm using Exc/Em slits of 5.0 nm/5.0 nm, respectively.

2.5. Docking

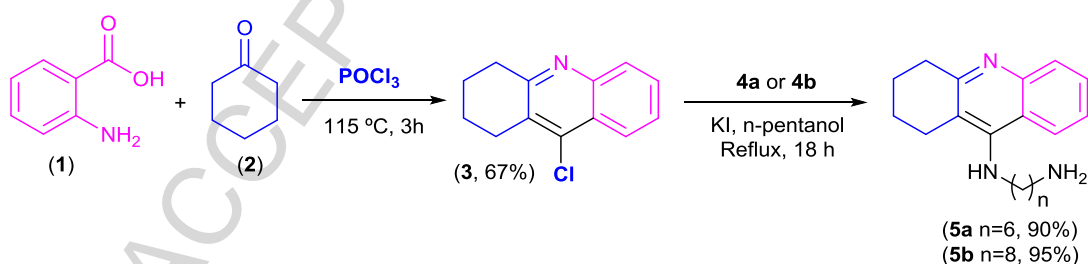
The BSA structure was obtained from the Protein Data Bank (<http://www.rcsb.org/pdb/>) with the ID: 4f5s [31]. The Chimera 1.8 software was used to remove the chain B [32], waters and other molecules, and added hydrogen atoms to the BSA protein. The ligands were built in the software

Avogadro 1.1.1 [33], following the semi empirical PM6 [34] geometry optimization using the program MOPAC2012 [35]. The ligands and protein in the pdbqt format were generated by AutoDockTools, where the ligands were considered flexible (with PM6 charges), and the BSA rigid (with Gasteiger charges) [36]. AutoDock Vina 1.1.1 program was used for the blind docking [37], using a gridbox of 94 x 62 x 86 and the coordinates $x = 9.46$, $y = 23.36$, $z = 98.15$, with an exhaustiveness of 150. As a model of binding pose, it was selected the compound's conformer with lowest binding free energy (ΔG). The results from docking were analyzed using the Accelrys Discovery Studio 3.5 software [38].

3. Results and Discussion

3.1. Synthesis

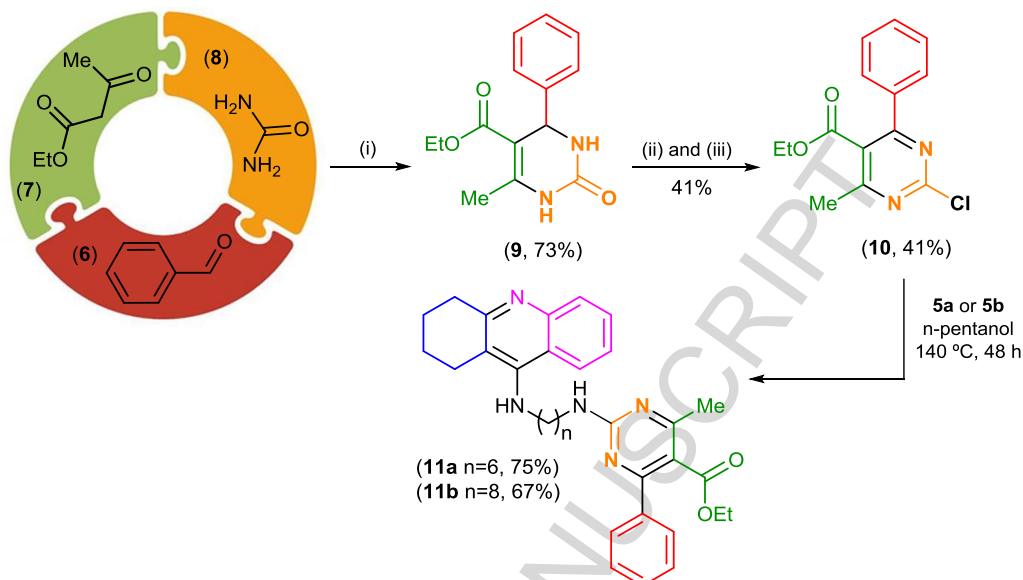
The classical Niementowski reaction between anthranilic acid (**1**) and cyclohexanone (**2**) mediated by POCl_3 provided the quinoline derivative 9-chloro-1,2,3,4-tetrahydroacridine (**3**) [24]. In sequence, treatment of the chloride with an excess of 1,6-diaminohexane (**4a**) or 1,8-diaminooctane (**4b**) under reflux for 18 h provided 9-amino-1,2,3,4-tetrahydroacridines **5a** and **5b**, as depicted in Scheme 1. This step was carried out in the presence of catalytic amount of KI [25].



Scheme 1. Preparation of Tacrine derivative precursors **5a-b**.

The Biginelli one-pot three component reaction between benzaldehyde (**6**), ethyl acetoacetate (**7**) and urea (**8**) in the presence of catalytic $\text{SnCl}_2 \cdot 2\text{H}_2\text{O}$ gave the DHPM **9** (Scheme 2) [26]. The following step was the selective oxidation of **9** with potassium persulfate followed by chlorination with POCl_3 , giving the pyrimidine ring in **10** [27,28]. Finally, the chloropyrimidine **10** was

reacted with amine **5a** and **5b** through an ipso-substitution giving the desired hybrids **11a** and **11b**, respectively (Scheme 2). The yields were 56% (**11a**) and 52% (**11b**).



Scheme 2. Preparation of Tacrine-pyrimidine hybrids from Biginelli reaction, where (i) $\text{SnCl}_2 \cdot 2\text{H}_2\text{O}$ (10%), Ethanol, 100 °C, 6 h. (ii) $\text{K}_2\text{S}_2\text{O}_8$, CH_3CN , H_2O , 73 °C, 80 min. (iii) POCl_3 , 115 °C, 30 min.

3.2. Photophysical properties

The photophysical investigation in solution (10^{-5} M) was carried out using different organic solvents with a wide range of dielectric constants (1,4-dioxane dichloromethane, ethanol, acetonitrile and dimethylsulfoxide). The relevant data from the electronic ground and excited states characterization in both steady-state and time-resolved spectroscopies are summarized in Tables 1-3.

Figure 2 shows the UV-Vis spectra of the isolated Tacrine (Figure 2a) and Biginelli DHPM **10** (Figure 2b), as well as the respective molecular hybrids **11a** (Figure 2c) and **11b** (Figure 2d). Tacrine presents absorption maxima below 350 nm depending on the solvent but with any clear tendency on the environment polarity, which can be related to an almost absent charge transfer character in the ground state. The Biginelli pyrimidine precursor present absorption maxima located between 275-278 nm, as expected due to its higher HOMO-LUMO energy gap, due to the lower electronic conjugation if compared

to the Tacrine. The respective molecular hybrids **11a** and **11b** present absorption maxima, similar to that observed for Tacrine, located in the range 319-334 nm. In this sense, it seems that the molecular hybrids keep mostly the electronic properties of Tacrine in the ground state. In addition, as already observed for similar molecular hybrids, the aliphatic chain length seems not affect at all the photophysics of these compounds in the ground state [17].

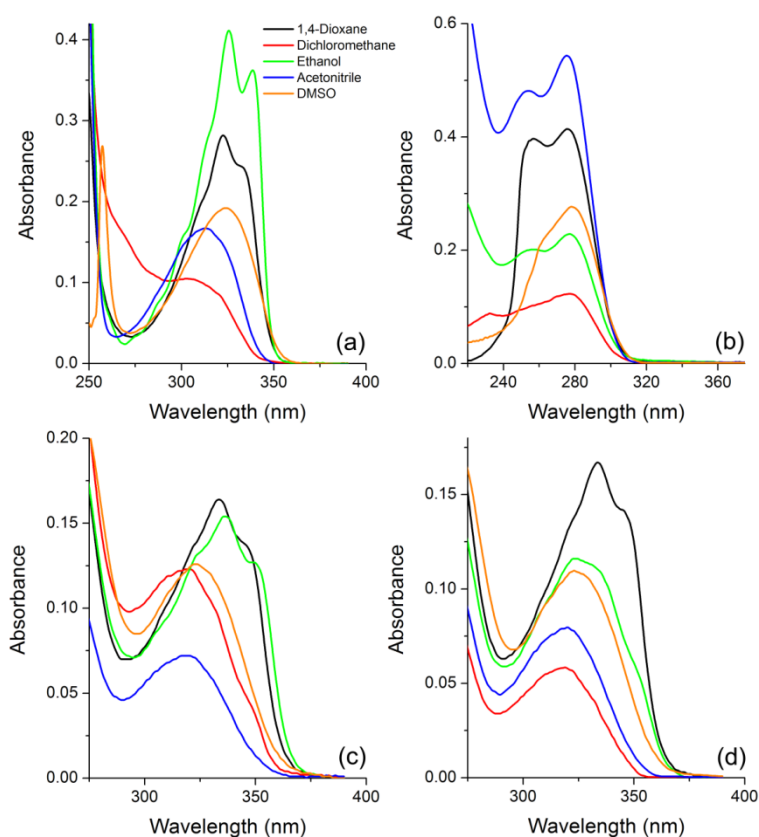


Figure 2. UV-Vis absorption spectra in solution of different organic solvents [ca. 10^{-5} M] of (a) Tacrine, (b) Biginelli DHPM **10** and molecular hybrids (c) **11a** and (d) **11b**.

In this study, the UV-Vis spectroscopy was also used to obtain the experimental extinction coefficient (ϵ) and the respective theoretical rate constant for emission (k_e^0), as well as the respective oscillator strengths (f_e) using Equation (1) [39]:

$$f_e \approx 4.3 \times 10^{-9} \int \epsilon d\bar{\nu} \quad (1)$$

For an electronic transition, Equation (1) relates the area under the absorption curve from a plot of the molar absorptivity coefficient ϵ ($M^{-1} \cdot cm^{-1}$) against

wavenumber $\bar{\nu}$ (cm^{-1}) with its oscillator strength (f_e). Moreover, from Equation (2) and using the same integral, the theoretical rate constant for emission (k_e^0) can be obtained, where the pure radiative lifetime τ^0 is defined as $1/k_e^0$ [40].

$$k_e^0 \approx 2.88 \times 10^{-9} \bar{\nu}_0^2 \int \epsilon d\bar{\nu} \quad (2)$$

In this regard, the molar absorptivity coefficient values (ϵ), as well as the calculated radiative rate constants (k_e^0) present in Table 1 indicate for all studied compounds, spin and symmetry allowed electronic transitions, which could be related to $^1\pi\pi^*$ transitions. In addition, an almost constant radiative lifetime indicates that after the radiation absorption the molecular hybrids populate the same excited state.

Table 1. Photophysical data of compounds from UV-Vis absorption spectroscopy, where ε is the molar extinction coefficient ($\times 10^4 \text{ M}^{-1} \cdot \text{cm}^{-1}$), λ_{abs} is the absorption maxima (nm), f_e is the calculated oscillator strength, k_e^0 is the calculated radiative rate constant (10^8 s^{-1}) and τ^0 is the calculated pure radiative lifetime (ns).

Compound	Solvent	λ_{abs} (nm)	ε ($\times 10^4 \text{ M}^{-1} \cdot \text{cm}^{-1}$)	f_e	k_e^0 (10^8 s^{-1})	τ^0 (ns)
Tacrine	1,4-Dioxane	323	1.40	0.22	1.42	7.05
	Dichloromethane	314	1.03	0.18	1.25	7.98
	Ethanol	325	1.37	0.19	1.14	8.80
	Acetonitrile	314	0.69	0.17	1.15	8.72
	Dimethylsulfoxide	326	0.81	0.16	1.02	9.84
10	1,4-Dioxane	275	1.80	0.32	2.81	3.55
	Dichloromethane	278	0.62	0.16	1.36	7.36
	Ethanol	277	1.13	0.20	1.77	5.65
	Acetonitrile	275	1.71	0.28	2.50	4.00
	Dimethylsulfoxide	278	1.30	0.26	2.25	4.44
11a	1,4-Dioxane	334	1.84	0.25	1.54	6.50
	Dichloromethane	319	0.91	0.17	1.11	9.00
	Ethanol	336	1.37	0.18	1.05	9.49
	Acetonitrile	321	0.97	0.16	1.08	9.23
	Dimethylsulfoxide	327	1.43	0.28	1.82	5.50
11b	1,4-Dioxane	334	1.67	0.23	1.41	7.07
	Dichloromethane	321	0.63	0.13	0.89	11.15
	Ethanol	328	1.10	0.18	1.13	8.82
	Acetonitrile	320	1.11	0.15	0.97	10.29
	Dimethylsulfoxide	324	1.21	0.18	1.17	8.53

The fluorescence emission curves were obtained by exciting the compounds at the absorption maxima (Table 1). The Tacrine precursor presents in all studied solvents a main fluorescence emission in the UV-A region (~375 nm). Biginelli DHPM **10** shows a very weak emission in the 250-500 nm region (see fluorescence quantum yields, Table 2). The molecular hybrids **11a** and **11b** present fluorescence emission around 380 nm, quite similar to the emission observed to pure Tacrine. Once more, the aliphatic chain length seems not affect at all the photophysics of these compounds. The fluorescence quantum yield of the Tacrine when compared to the respective hybrids, probably indicates that the vibrational relaxation seems to play a fundamental role on the deactivation of the excited state, different than observed for similar molecular hybrids [17].

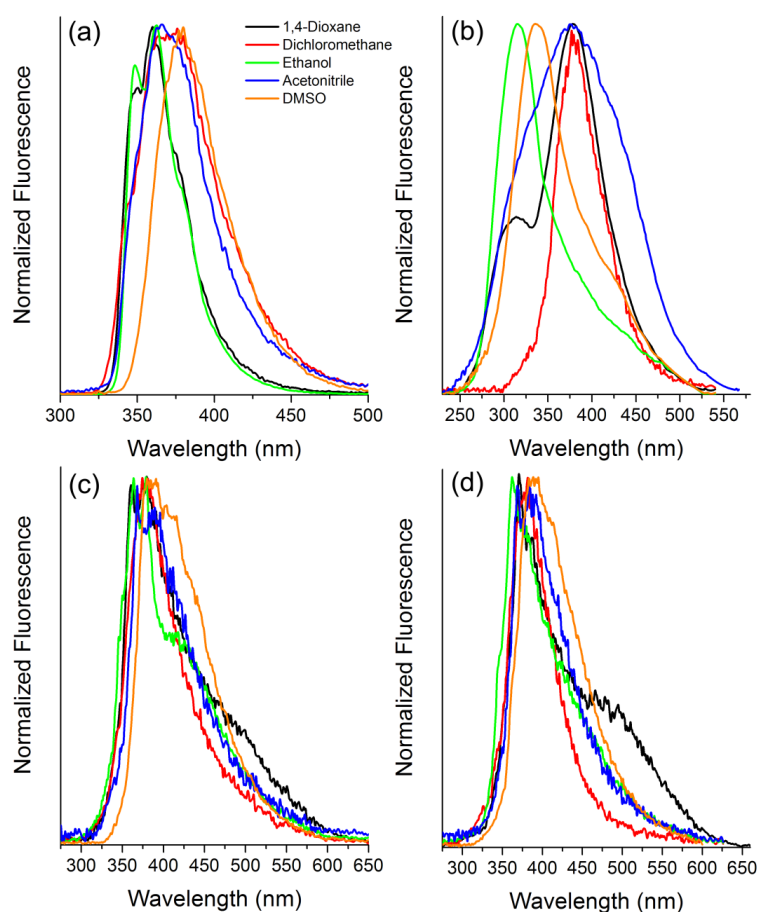


Figure 3. Steady-state fluorescence emission spectra in solution of different organic solvents [ca. 10^{-5} M] of (a) Tacrine, (b) Biginelli DHPM **10** and molecular hybrids (c) **11a** and (d) **11b**.

Table 2. Photophysical data from steady-state fluorescence emission spectroscopy of precursors Tacrine and Biginelli DHPM **10** and respective molecular hybrids **11a-b**, where λ_{em} is the emission maxima, $\Delta\lambda_{ST}$ is the Stokes shift (nm/cm⁻¹) and ϕ_{FL} is the fluorescence quantum yield.

Compound	Solvent	λ_{em} (nm)	$\Delta\lambda_{ST}$ (nm/cm ⁻¹)	ϕ_{FL}
Tacrine	1,4-Dioxane	359	36/3105	0.02
	Dichloromethane	374	60/5109	0.04
	Ethanol	362	37/3145	0.23
	Acetonitrile	368	54/4673	0.02
	Dimethylsulfoxide	379	53/4290	0.23
10	1,4-Dioxane	378	103/9909	<0.01
	Dichloromethane	378	100/9516	<0.01
	Ethanol	306	29/3421	<0.01
	Acetonitrile	378	103/9908	<0.01
	Dimethylsulfoxide	334	56/6031	<0.01
11a	1,4-Dioxane	378	44/3485	0.02
	Dichloromethane	378	59/4893	0.01
	Ethanol	371	35/2808	0.01
	Acetonitrile	380	59/4837	<0.01
	Dimethylsulfoxide	385	58/4607	0.01
11b	1,4-Dioxane	380	46/3624	<0.01
	Dichloromethane	380	59/4837	<0.01
	Ethanol	372	44/3606	<0.01
	Acetonitrile	382	62/5072	<0.01
	Dimethylsulfoxide	388	64/5091	<0.01

Based on the steady-state results, time-resolved fluorescence was also employed to better understand the photophysics of the molecular hybrids **11a** and **11b** (Figure 3). The relevant data are summarised in Table 3 and the respective residuals are presented in the ESI. The fluorescence decay profile of Tacrine could be fitted with good χ^2 values, showing bi-exponential decay with higher contribution (> 90%) from the shorter time decay (0.115-0.207 ns) in despite the longer one (2.468-2.543 ns) allowing the calculation of an averaged time decay below 0.3 ns. On the other hand, the DHPM precursor **10** presented mono-exponential decays with values ranging 0.212-0.601 ns. Similarly, the molecular hybrids showed mono-exponential decays, being closer to the longer lifetime of Tacrine. In addition, it could also be observed that the solvent does

not affect significantly the fluorescence lifetimes of the precursors and respective hybrids. The individual curves, as well as the respective residuals are presented in the supporting information.

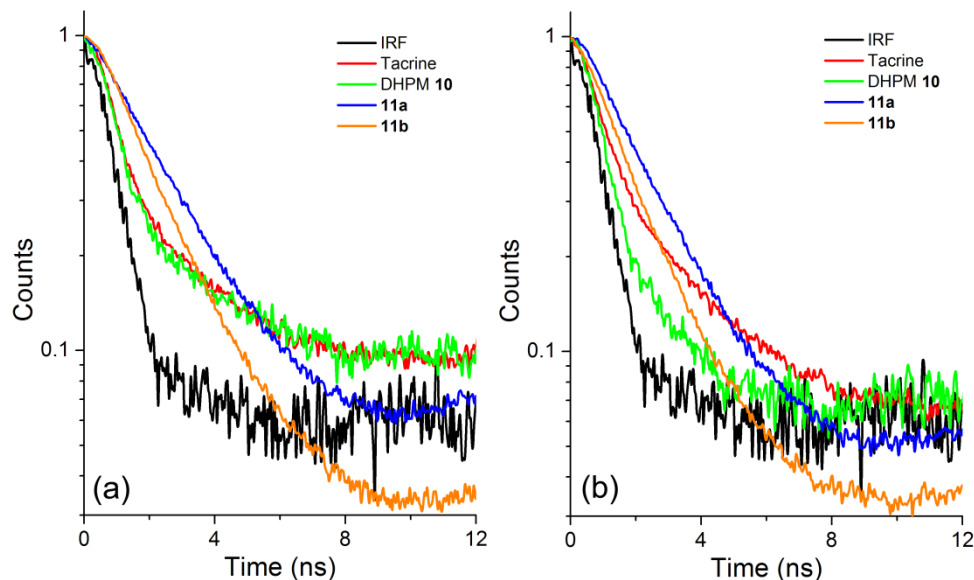


Figure 4. Time-resolved fluorescence decays of molecular hybrids **11a** and **11b** in (a) 1,4-dioxane and (b) acetonitrile ($\sim 10^{-5}$ M). The precursors Tacrine and Biginelli DHPM **10** were also presented for comparison. IRF=instrument response factor.

Table 3. Selected data from the time resolved fluorescence emission of Tacrine, DHPM **10** and molecular hybrids **11a** and **11b**, where τ is the experimental fluorescence lifetime (in ns), τ_{av} is the fluorescence lifetime average (in ns) and χ^2 represents the quality of the fit.

Compound	Solvent	τ_1 (ns) (%)	τ_2 (ns) (%)	τ_{av} (ns)	χ^2
Tacrine	1,4-Dioxane	0.115 (97.6)	2.543 (2.4)	0.173	1.147
	Acetonitrile	0.207 (93.6)	2.468 (6.4)	0.351	1.050
10	1,4-Dioxane	0.601 (100)	-	0.601	1.092
	Acetonitrile	0.212 (100)	-	0.212	1.039
11a	1,4-Dioxane	1.851 (100)	-	1.851	1.073
	Acetonitrile	1.642 (100)	-	1.642	1.199
11b	1,4-Dioxane	1.389 (100)	-	1.389	1.145
	Acetonitrile	1.261 (100)	-	1.261	1.193

3.3 BSA interaction study

It is described in the literature to the BSA in buffered solution, an absorption and an intrinsic fluorescence emission maxima located at 280 nm and 340 nm, respectively, with latter due to tryptophan residues [19]. In this sense, and based on the photophysical properties of the molecular hybrids, BSA interaction with the molecular hybrids **11a** and **11b** was studied from the fluorescence quenching of BSA, focusing on the suppression experiment and also based on the increase on the fluorescence emission of the fluorophore, related to the association study. In this investigation, the photophysics of both precursors Tacrine and DHPM **10** were also evaluated for comparison.

The first set of experiments regarding the BSA suppression was performed to the pure precursor Tacrine as showed in Figure 5. The Tacrine and DHPM **10** present in PBS media and in absence of BSA absorption bands around 325 and 275 nm, respectively (data not shown, see Supporting information). It can be observed that upon addition of the Tacrine into the solution containing BSA, the UV-Vis absorption band around 275 nm spectra seems almost constant (BSA absorption band), with significative increase on the absorption intensities at ~325 nm ascribed to the Tacrine absorption were observed, as expected (Figure 5a). The fluorescence emission spectra of BSA (Figure 5b) shows an almost constant intensity with an F_0/F ratio close to unity in relation to the dye concentration (see Figure 5b, insert). This result indicates that contrary to that observed for DHPM **10**, tacrine shows no significant interaction with BSA that would result in the suppression of its fluorescence. It is worth mentioning that the interaction between the precursor DHPM **10** and BSA was already studied in the literature, where it could be observed that the absorption between 250 and 300 nm increases after addition of the precursor **10**, as expected, with significant decrease in the fluorescence intensity of BSA [17]. In addition, any association of the precursors with BSA, related to increase of the fluorescence intensity of the precursors could be observed (data not shown, see ESI Figures S7-S10).

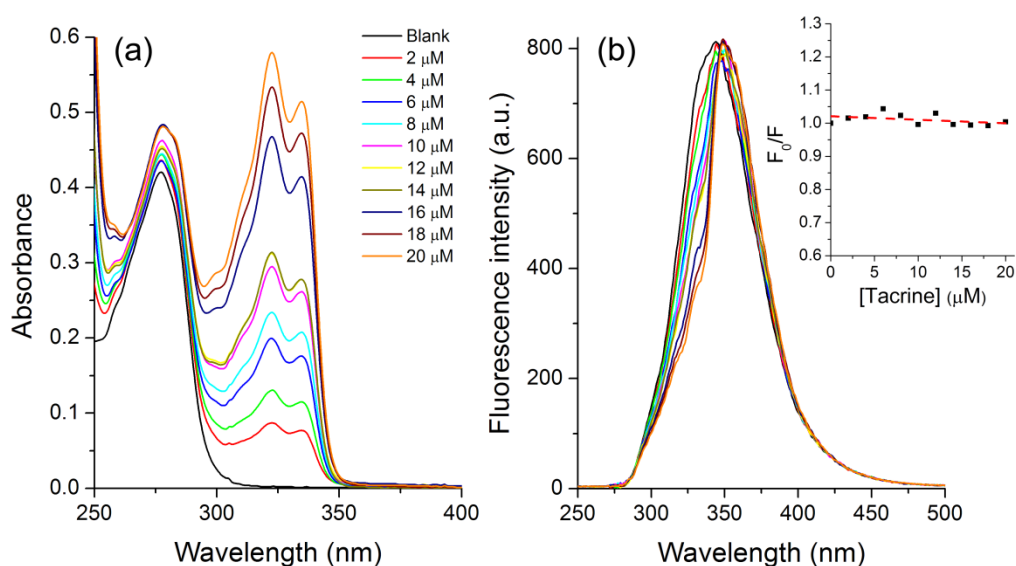


Figure 5. (a) UV-Vis absorption and (b) fluorescence emission spectra ($\lambda_{\text{exc}}=277$ nm) of BSA in PBS solution in the presence of different amounts of Tacrine **1**. The blank sample is the pure BSA. The inset presents the Stern-Volmer relation.

On the other hand, as observed in Figure 6, the addition of the molecular hybrids **11a** and **11b** increases the absorption intensity in the region between 300-375 nm, as expected. However, different than observed to the Tacrine, a significant decrease on the fluorescence intensity of the BSA takes place after addition of **11a** and **11b**.

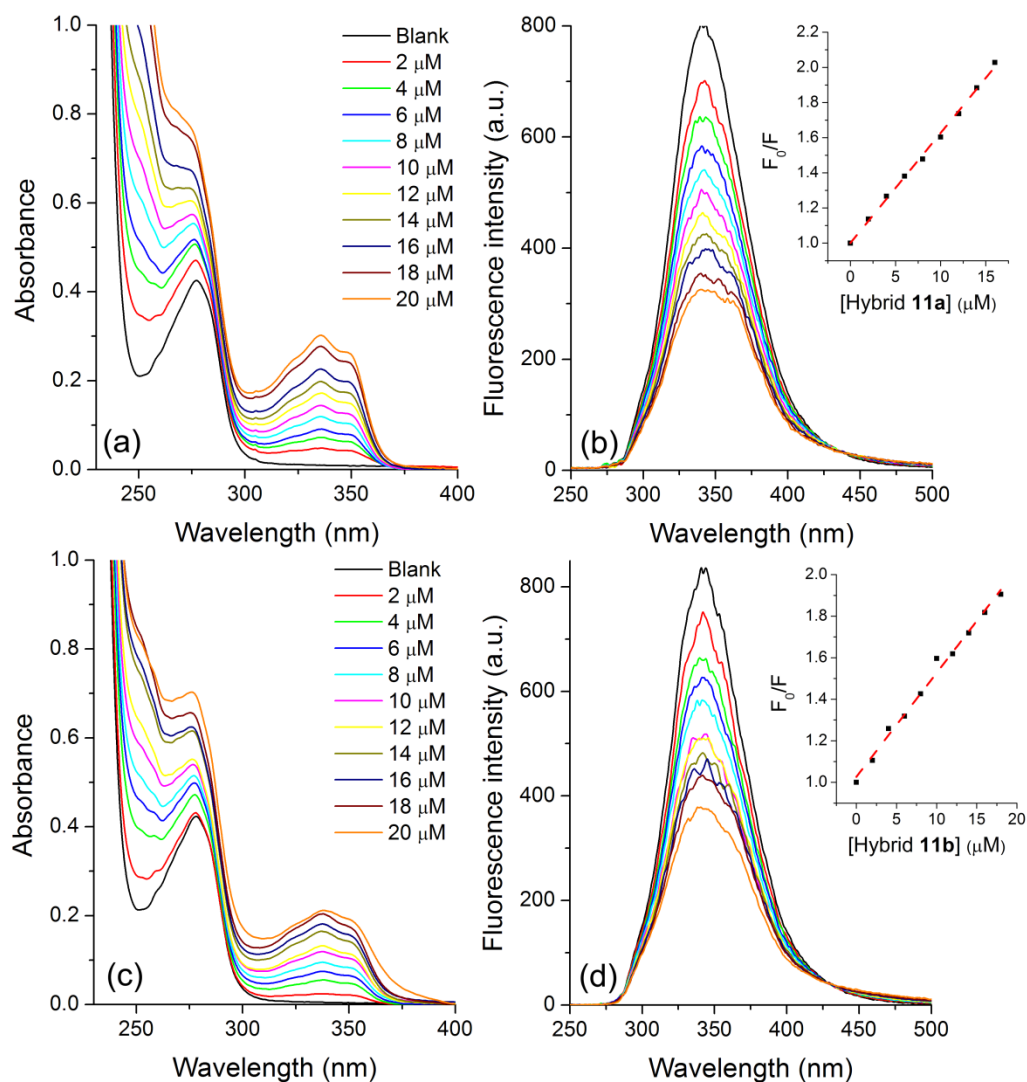


Figure 6. UV-Vis absorption and fluorescence emission spectra ($\lambda_{\text{exc}}=277$ nm) of BSA in PBS solution in the presence of different amounts of **11a** (top) and **11b** (bottom). The blank sample is the pure BSA. The inserts present the respective Stern-Volmer relations.

Based on the photophysical results of the BSA in presence of the molecular hybrids, the fluorescence quenching of the BSA could be evaluated using the Stern-Volmer relation presented in Equation (3) [41].

$$F_0/F = 1 + K_{\text{SV}}[Q] = 1 + K_q\tau_0[Q] \quad (3)$$

In Equation (3), F_0 and F , are the fluorescence intensities of the BSA in the absence and presence of the quencher, respectively, K_{SV} is

the Stern-Volmer constant and $[Q]$ is the quencher concentration. In addition, K_{SV} can be related to the product of a bimolecular suppression constant K_q and the fluorophore lifetime in absence of the quencher τ_0 , with the latter presenting usually values around 10^{-8} s to biomolecules (Figure 6, inserts) [41]. The molecular hybrids presented values to the K_{SV} of $6.26 \times 10^4 \text{ M}^{-1}$ (**11a**) and $5.00 \times 10^4 \text{ M}^{-1}$ (**11b**), which are quite close to the values observed to the pure DHPM **10** ($6.63 \times 10^4 \text{ M}^{-1}$) [17], indicating that the pyrimidine moiety is playing an important role on the efficient BSA quenching. Yet, the methylene chain seems not to affect the interaction between BSA and quencher. As already discussed in this study, due to the fluorophore lifetime ($\tau_0 \sim 10^{-8}$ s), the bimolecular suppression constant K_q of the molecular hybrids for BSA were calculated to be $6.26 \times 10^{12} \text{ M}^{-1} \cdot \text{s}^{-1}$ (**11a**) and $5.00 \times 10^{12} \text{ M}^{-1} \cdot \text{s}^{-1}$ (**11b**). The calculated values for K_q exceed the maximum values to the diffusional mechanism ($2.0 \times 10^{10} \text{ M}^{-1} \cdot \text{s}^{-1}$), it can be concluded that the nature of quenching is not dynamic but probably static, resulting in forming molecular hybrids-BSA complexes in the ground state [42]. Taking the static approach into account, it is also possible to calculate the binding constant (K_a) and the respective number of binding sites (n) between the BSA and the suppressor by applying the Scatchard relation presented in Equation (4) [43].

$$\log [(F_0 - F)/F] = \log K_a + n \log [Q] \quad (4)$$

In Figure 7, it is presented the double logarithmic plot relating the fluorescence intensities from the BSA and the quenchers concentration. For both molecular hybrids, it can be observed a linear plot correlation with comparable binding constants (K_a) of 2.95×10^4 (**11a**) and 3.63×10^4 (**11b**) with only one binding site for molecular hybrids **11a** ($n=0.94$) and **11b** ($n=0.95$). Once again, this result indicates that the methylene linker does not play a significant role on the molecular hybrids interaction with the BSA.

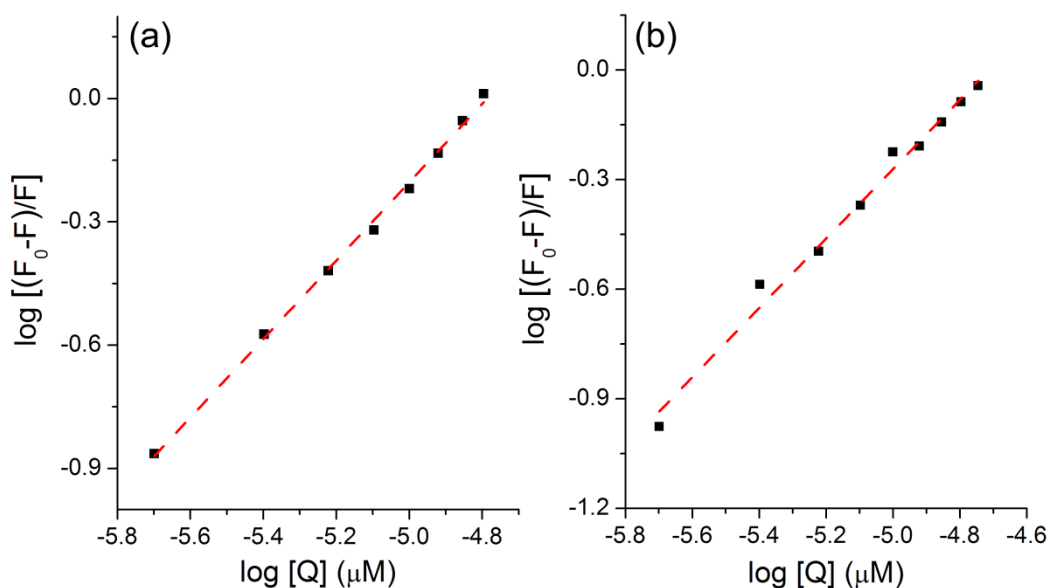


Figure 7. Log-log plot of BSA fluorescence intensities vs. molecular hybrids **11a** (a) and **11b** (b) concentrations [Q] used to obtain the binding constant (K_a) and binding sites (n) using Equation (4).

3.4 Molecular Modelling of BSA with hybrids

To better understand the binding modes of Tacrine, DHPM **10** and hybrids **11a** and **11b** in the BSA protein, molecular docking simulations were carried out. According to the docking, the molecules interacted in different binding sites. The Tacrine bound in the IIA domain, **10** and **11a** molecules interacted in the IB domain, while the **11b** compound bound between the IB and IIIA domains of BSA (**Figure 8a**). The Tacrine interacted close with the Trp213 residue, presenting H-bonds with the Arg256 and hydrophobic interactions with Leu237, His241 and Ile289 residues (**Figure 8b**). The compound **10** bound in the region close to the Trp134 residue, interacts with the Pro117, Ile181, Tyr160 and Ile141 residues by hydrophobic interactions (**Figure 8c**). The compound **11a** demonstrated hydrophobic interactions with the Pro117, Leu122, Leu115 (in the pyrimidine moiety) and Leu189 (in the Tacrine group) residues and an H-bond with the Arg185 (in the Tacrine moiety) (**Figure 8d**). The **11b** hybrid showed hydrophobic interactions with the Ile181 (in the Tacrine moiety) and the Leu189 (in the pyrimidine group) residues, H-bonds with the Arg458 and Ser192 (in the pyrimidine group), and electrostatic interactions with the Glu424, Arg458 (in the pyrimidine moiety) and Arg158 (in the Tacrine group) residues (**Figure 8e**).

Despite the hybrids molecules (**11a** and **11b**) presented a binding pose practically in the same site of **10**, the pyrimidine moiety showed different conformations and interactions. The insertion of the carbon chain (linker) and the Tacrine moiety in **11a** and **11b** caused a change in the binding pose of them. The compounds **10**, **11a** and **11b** are 11.5-13.5 Å of distance from the Trp134, while the Tacrine is 3.8 Å from the Trp213 residue. The interaction of the compounds in these regions could lead a conformational change in BSA and consequently affect the Trp fluorescence quenching. [44,45,46,47,48,49] Moreover, the predicted binding energy (ΔG_{bind}) obtained from molecular docking indicated that Tacrine, **10**, **11a** and **11b**, interacts spontaneously with the BSA ($\Delta G = -8.2$; -6.9 ; -9.3 ; and -9.7 kcal·mol⁻¹, respectively). These results could indicate that the molecular hybrids **11a** and **11b** may have a better affinity for BSA than the Tacrine and DHPM **10**. Previous studies have indicated that these BSA regions are binding sites of molecules and could be involved in the fluorescence quenching [44,45,46,50,51].

In addition, is important to mention that despite the short distance between the Trp213 residue and the tacrine, obtained from the molecular docking simulations, this molecule does not show significant suppression of the BSA fluorescence. Probably, the orientation between the donor (Trp residue) and the acceptor (Tacrine) is interfering in the fluorescence quenching.[48] In fact, a π - π interaction, which could indicate a good orientation,[52,53] was not observed here. In relation to the hybrids molecules, the distances between them and the Trp134 (11.5-13.5 Å) are in accordance with previous studies (9-24 Å),[54,55,56] where also were observed the BSA fluorescence quenching.

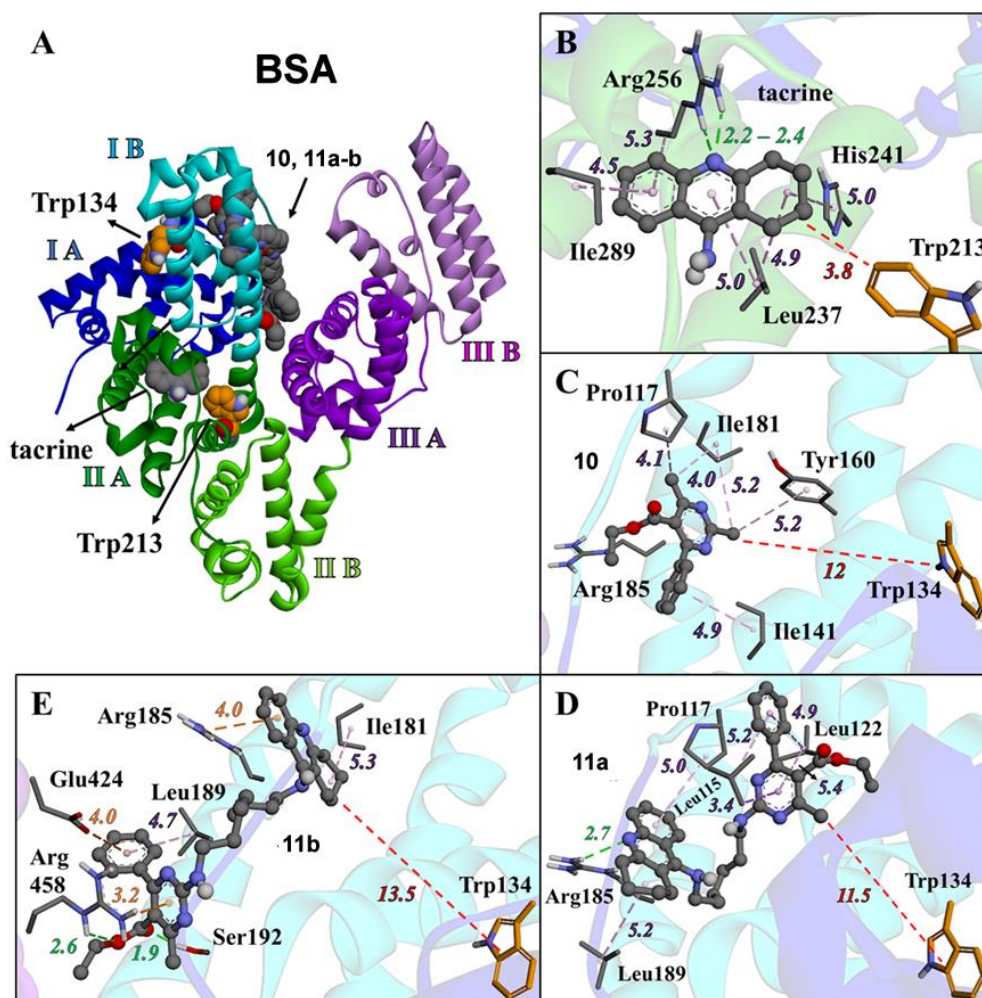


Figure 8. Docking simulations between the BSA protein (a) and the Tacrine (b), DHPM **10** (c) and molecular hybrids **11a** (d) and **11b** (e). The H-bonds, hydrophobic (π -alkyl, π - π T-shaped) and electrostatic (π -anion and π -cation), interactions are shown in green, orange and purple dot lines, respectively. Red dot lines represent the distances (in Å) between the molecules and the Trp residues. The BSA domains I A (1-112); I B (113-195); II A (196-303); II B (304-383); III A (384-500) and III B (501-583), were based on reports of Ramezani et al. [57] and Wang et al. [58].

4. Conclusion

In summary, two new molecular hybrids containing Tacrine and Biginelli pyrimidine connected by a methylene linker were synthesized by multicomponent reaction in good yields (67-75%). The molecular hybrids presented absorption around 320 nm, close to the Tacrine absorption. The compounds also presented fluorescence emission around 400 nm, as observed

for the separate Tacrine and pyrimidine structures. The photophysical results showed an almost absent influence of the solvent on absorption or emission maxima location. Although pure Tacrine did not presented any interaction with BSA, both molecular hybrids showed BSA suppression properties due to the pyrimidine moiety, with relative large values to the Stern-Volmer ($\sim 10^4 \text{ M}^{-1}$) and bimolecular suppression ($\sim 10^{12} \text{ M}^{-1} \cdot \text{s}^{-1}$) constants. Docking indicated that the molecular hybrids presented better affinity for BSA than the isolated precursor Tacrine and Biginelli pyrimidine. Finally, photoactive molecular hybrids seems to be a powerful tool to design new optical sensors for biomolecules in solution, where the synergy between their photophysical properties and specific functional groups can be found.

Conflict of interests

The authors have declared no conflict of interest.

Acknowledgements

The authors would like to acknowledge FAPERGS (17/2551-0000968-1), CNPq (409855/2018-9) and Coordenação de Aperfeiçoamento de Pessoal de Nível Superior - Brasil (CAPES) - Finance Code 001 for the financial support.

References

-
- [1] Y. Suzuki, K. Yokoyama, Development of functional fluorescent molecular probes for the detection of biological substances, *Biosensors* 5 (2015) 337-363.
 - [2] J.W. Lichtman, J.A. Conchello, Fluorescence microscopy, *Nat. Methods* 2 (2005) 910-919.
 - [3] D.J. Stephens, V.J. Allan, Light microscopy techniques for live cell Imaging, *Science* 300 (2003) 82-86.
 - [4] H. Kobayashi, M. Ogawa, R. Alford, P.L. Choyke, Y. Urano, New strategies for fluorescent probe design in medical diagnostic imaging, *Chem. Rev.* 110 (2010) 2620-2640.
 - [5] M. Liu, R.Z. Li, Y. Tang, J.W. Chang, R. Han, S.M. Zhang, N. Jiang, F.L. Ma, New applications of the Acridine Orange fluorescence staining method: Screening for circulating tumor cells, *Oncol. Lett.* 13 (2017) 2221-2229.

- [6] K.A.P. Sousa, F.M.R. Lima, T.O. Monteiro, S.M. Silva, M.O.F. Goulart, F.S. Damos, R.D.S. Luz, Amperometric photosensor based on Acridine Orange/TiO₂ for Chlorogenic Acid determination in food samples, *Food. Anal. Methods.* 11 (2018) 2731-2741.
- [7] B. Czaplinska, E. Spaczynska, R. Musiol, Quinoline fluorescent probes for zinc - from diagnostic to therapeutic molecules in treating neurodegenerative diseases, *Med. Chem.* 14 (2018) 19-33.
- [8] C.Y. Wang, J.X. Fu, K. Yao, K. Xue, K.X. Xu, X.B. Pang, Acridine-based fluorescence chemosensors for selective sensing of Fe³⁺ and Ni²⁺ ions, *Spectrochim. Acta A* 199 (2018) 403-411.
- [9] A. Milelli, A. De Simone, N. Ticchi, H.H. Chen, N. Betari, V. Andrisano, V. Tumiatti, Tacrine-based multifunctional agents in Alzheimer's disease: An old story in continuous development, *Curr. Med. Chem.* 24 (2017) 3522-3546.
- [10] B. Sameem, M. Saeedi, M. Mahdavi, A. Shafiee, A review on Tacrine-based scaffolds as multi-target drugs (MTDLs) for Alzheimer's disease, *Eur. J. Med. Chem.* 128 (2017) 332-345.
- [11] M.A. Ceschi, J.S. da Costa, J.P.B. Lopes, V.S. Camara, L.F. Campo, A.C.D. Borges, C.A.S. Goncalves, D.F. de Souza, E.L. Konrath, A.L.M. Karl, I.A. Guedes, L.E. Dardenne, Novel series of Tacrine-Tianeptine hybrids: Synthesis, cholinesterase inhibitory activity, S10013 secretion and a molecular modeling approach, *Eur. J. Med. Chem.* 121 (2016) 758-772.
- [12] J.P.B. Lopes, J.S. da Costa, M.A. Ceschi, C.A.S. Goncalves, E.L. Konrath, A.L.M. Karl, I.A. Guedes, L.E. Dardenne, Chiral bistacrine analogues: synthesis, cholinesterase inhibitory activity and a molecular modeling approach, *J. Braz. Chem. Soc.* 28 (2017) 2218-2228.
- [13] J.P.B. Lopes, L. Silva, G.D. Franarin, M.A. Ceschi, D.S. Ludtke, R.F. Dantas, C.M.C. de Salles, F.P. Silva, M.R. Senger, I.A. Guedes, L.E. Dardenne, Design, synthesis, cholinesterase inhibition and molecular modelling study of novel Tacrine hybrids with carbohydrate derivatives, *Bioorg. Med. Chem.* 26 (2018) 5566-5577.
- [14] A. de Fatima, T.C. Braga, L.D. Neto, B.S. Terra, B.G.F. Oliveira, D.L. da Silva, L.V. Modolo, A mini-review on Biginelli adducts with notable pharmacological properties, *J. Adv. Res.* 6 (2015) 363-373.

- [15] N.A. Al-Masoudi, N.J. Al-Salihi, Y.A. Marich, T. Markus, Synthesis and fluorescence properties of new Monastrol analogs conjugated fluorescent coumarin scaffolds, *J. Fluoresc.* 26 (2016) 31-35.
- [16] V.P. de Souza, V. Vendrusculo, A.M. Moras, L. Steffens, F.S. Santos, D.J. Moura, F.S. Rodembusch, D. Russowsky, Synthesis and photophysical study of new fluorescent proton transfer dihydropyrimidinone hybrids as potential candidates for molecular probes, *New J. Chem.* 41 (2017) 15305-15311.
- [17] J.P.B. Lopes, V.S. Câmara, D. Russowsky, F.d.S. Santos, R. Beal, P.A. Nogara, J.B.T. da Rocha, P.F.B. Gonçalves, F.S. Rodembusch, M.A. Ceschi, Lophine and pyrimidine based photoactive molecular hybrids. Synthesis, photophysics, BSA interaction and DFT study, *New J. Chem.* 42 (2018) 17126 - 17137.
- [18] E.L. Gelamo, C. Silva, H. Imasato, M. Tabak, Interaction of bovine (BSA) and human (HSA) serum albumins with ionic surfactants: spectroscopy and modelling, *BBA-Protein Struct. M.* 1594 (2002) 84-99.
- [19] A. Sulkowska, Interaction of drugs with bovine and human serum albumin, *J. Mol. Struct.* 614 (2002) 227-232.
- [20] J. Wang, Y.Y. Zhang, Y. Guo, L. Zhang, R. Xu, Z.Q. Xing, S.X. Wang, X.D. Zhang, Interaction of bovine serum albumin with Acridine Orange (CI Basic Orange 14) and its sonodynamic damage under ultrasonic irradiation, *Dyes Pigm.* 80 (2009) 271-278.
- [21] L.B. Chen, M.H. Wu, X.C. Lin, Z.H. Xie, Study on the interaction between human serum albumin and a novel bioactive acridine derivative using optical spectroscopy, *Luminescence* 26 (2011) 172-177.
- [22] J. Zhang, D.X. Xiong, L.N. Chen, Q.L. Kang, B.R. Zeng, Interaction of pyrrolizine derivatives with bovine serum albumin by fluorescence and UV-Vis spectroscopy, *Spectrochim. Acta A* 96 (2012) 132-138.
- [23] X.Z. Feng, Z. Lin, L.J. Yang, C. Wang, C.L. Bai, Investigation of the interaction between Acridine Orange and bovine serum albumin, *Talanta* 47 (1998) 1223-1229.
- [24] M.K. Hu, L.J. Wu, G. Hsiao, M.H. Yen, Homodimeric Tacrine congeners as acetylcholinesterase inhibitors, *J. Med. Chem.* 45 (2002) 2277-2282.

- [25] W. Luo, Y.P. Li, Y. He, S.L. Huang, J.H. Tan, T.M. Ou, D. Li, L.Q. Gu, Z.S. Huang, Design, synthesis and evaluation of novel tacrine-multialkoxybenzene hybrids as dual inhibitors for cholinesterases and amyloid beta aggregation, *Bioorg. Med. Chem.* 19 (2011) 763-770.
- [26] D. Russowsky, F.A. Lopes, V.S.S. da Silva, K.F.S. Canto, M.G.M. D'Oca, M.N. Godoi, Multicomponent Biginelli's synthesis of 3,4-dihydropyrimidin-2(1H)-ones promoted by SnCl₂·2H₂O, *J. Braz. Chem. Soc.* 15 (2004) 165-169.
- [27] K. Singh, B.J. Wan, S. Franzblau, K. Chibale, J. Balzarini, Facile transformation of Biginelli pyrimidin-2(1H)-ones to pyrimidines. In vitro evaluation as inhibitors of Mycobacterium tuberculosis and modulators of cytostatic activity, *Eur. J. Med. Chem.* 46 (2011) 2290-2294.
- [28] H.R. Memarian, A. Farhadi, Potassium peroxydisulfate as an efficient oxidizing agent for conversion of ethyl 3,4-dihydropyrimidin-2(1h)-one-5-carboxylates to their corresponding ethyl pyrimidin-2(1h)-one-5-carboxylates, *J. Iran Chem. Soc.* 6 (2009) 638-646.
- [29] I.B. Berlan, *Handbook of Fluorescence Spectra of Aromatic Molecules*, 2nd ed. Academic Press, NY, 1971.
- [30] C. Würth, M. Grabolle, J. Pauli, M. Spieles and U. Resch-Genger, Relative and absolute determination of fluorescence quantum yields of transparent samples, *Nat. Protoc.* 8 (2013) 1535-1550.
- [31] A. Bujacz, Structures of bovine, equine and leporine serum albumin, *Acta Crystallogr. Sect. D.* 68 (2012) 1278-1289.
- [32] E.F. Pettersen, T.D. Goddard, C.C. Huang, G.S. Couch, D.M. Greenblatt, E.C. Meng, T.E. Ferrin, UCSF Chimera--a visualization system for exploratory research and analysis, *J. Comput. Chem.* 25 (2004) 1605-1162.
- [33] M.D. Hanwell, D.E. Curtis, D.C. Lonie, T. Vandermeersch, E. Zurek, G.R. Hutchison, Avogadro: an advanced semantic chemical editor, visualization, and analysis platform, *J. Cheminform.* 4 (2012) 1-17.
- [34] J.J. Stewart, Optimization of parameters for semiempirical methods V: modification of NDDO approximations and application to 70 elements, *J. Mol. Mod.* 13 (2007) 1173-1213.
- [35] J.J. Stewart, MOPAC2012, 2012. Stewart Computational Chemistry. Colorado Springs, CO, USA. <http://OpenMOPAC.net>.

- [36] G.M. Morris, R. Huey, W. Lindstrom, M.F. Sanner, R.K. Belew, D.S. Goodsell, A.J. Olson, AutoDock4 and AutoDockTools4: Automated docking with selective receptor flexibility, *J. Comput. Chem.* 30 (2009) 2785-2791.
- [37] O. Trott, A.J. Olson, AutoDock Vina: improving the speed and accuracy of docking with a new scoring function, efficient optimization and multithreading, *J. Comput. Chem.* 31 (2010) 455-461.
- [38] Dassault Systèmes BIOVIA, Discovery Studio Modeling Environment, Release 2017, San Diego: Dassault Systèmes, 2017.
- [39] S.J. Strickler, R.A. Berg, Relationship between absorption intensity and fluorescence lifetime of molecules, *J. Chem. Phys.* 37 (1962) 814-822.
- [40] N.J. Turro, J.C. Scaiano, V. Ramamurthy, Principles of Molecular Photochemistry: An Introduction, University Science Book, 1st edn, 2008.
- [41] J.R. Lakowicz. In: Principles of Fluorescence Spectroscopy. 3rd ed. New York: Springer; 2006.
- [42] J.G. Xu, Z.B. Wang, In: Fluorimetry. 3rd ed., Science Press, Beijing, 2006.
- [43] G. Scatchard, The attraction of proteins for small molecules and ions, *Ann. New York Acad. Sci.* 51 (1949) 660-672.
- [44] S.K. Riyazuddeen, Probing of the binding profile of anti-hypertensive drug, captopril with bovine serum albumin: A detailed calorimetric, spectroscopic and molecular docking studies, *J. Chem. Thermodyn.* 126 (2018) 43-53.
- [45] M.U. Mir, J.K. Maurya, S. Ali, S. Ubaid-ullah, A.B. Khan, R. Patel, Molecular interaction of cationic gemini surfactant with bovine serum albumin: A spectroscopic and molecular docking study, *Process. Biochem.* 49 (2014) 623-360.
- [46] L. Satish, S. Millan, V.V. Sasidharan, H. Sahoo, Molecular level insight into the effect of triethyloctylammoniumbromide on the structure, thermal stability, and activity of Bovineserum albumin, *Int. J. Biol. Macromol.* 107 (2018) 186-193.
- [47] M.S. Ali, H.A. Al-Lohedan, Experimental and computational investigation on the molecular interactions of Safranal with bovine serum albumin: Binding and anti-amyloidogenic efficacy of ligand, *J. Mol. Liq.* 278 (2019) 385-393.

- [48] A.B.T. Ghisaidoobe, S.J. Chung, Intrinsic tryptophan fluorescence in the detection and analysis of proteins: A focus on Förster Resonance Energy Transfer techniques, *Int. J. Mol. Sci.* 15 (2014) 22518-22538.
- [49] C. Hao, G. Xu, Y. Feng, L. Lu, W. Sun, R. Sun, Fluorescence quenching study on the interaction of ferroferric oxide nanoparticles with bovine serum albumin, *Spectrochim. Acta A Mol. Biomol. Spectrosc.* 184 (2017) 191-197.
- [50] J. Zhang, W. Chen, B. Tang, W. Zhang, L. Chen, Y. Duan, Y. Zhu, Y. Zhu, Y. Zhang, Interactions of 1-hydroxypyrene with bovine serum albumin: insights from multi-spectroscopy, docking and molecular dynamics simulation methods, *RSC Adv.* 6 (2016) 23622-23633.
- [51] D. Biswal, N.R. Pramanik, S. Chakrabarti, M.G.B. Drew, K. Acharya, S. Chandra, Syntheses, crystal structures, DFT calculations, protein interaction and anticancer activities of water soluble dipicolinic acid-imidazole based oxidovanadium(IV) complexes, *Dalton. Trans.* 46 (2017) 16682-16702.
- [52] Y.H. Jiao, F.Y. Meng, G.B. Zhu, L.Z. Ran, Y.F. Jiang, Q. Zhang, Synthesis of a novel p-hydroxycinnamic amide with anticancer capability and its interaction with human serum albumin, *Exp. Ther. Med.* 17 (2019) 1321-1329.
- [53] M. Ikeda, M. Ueda-Wakagi, K. Hayashibara, R. Kitano, M. Kawase, K. Kaihatsu, N. Kato, Y. Suhara, N. Osakabe, H. Ashida, Substitution at the C-3 position of catechins has an influence on the binding affinities against serum albumin, *Molecules* 22 (2017) E314.
- [54] M. Mukherjee, P.S. Sardar, S.K. Ghorai, S.K. Samanta, A.S. Roy, S. Dasgupta, S. Ghosh, A comparative study of interaction of tetracycline with several proteins using time resolved anisotropy, phosphorescence, docking and FRET, *PLoS One* 8 (2013) e60940.
- [55] H.G. Bonacorso, T.P. Calheiro, T.V. Acunha, B.A. Iglesias, S.Z. Franceschini, A. Ketzer, A.R. Meyer, P.A. Nogara, J.B.T. Rocha, N. Zanatta, M.A.P. Martins, Novel aryl(heteroaryl)-substituted (pyrimidyl)benzamide-based BF₂ complexes: Synthesis, photophysical properties, BSA-binding, and molecular docking analysis, *Dyes Pigm.* 161 (2019) 396-402.
- [56] E. Rahnama, M. Mahmoodian-Moghaddam, S. Khorsand-Ahmadi, M.R. Saberi, J. Chamani, Binding site identification of Metformin to human serum albumin and glycosylated human serum albumin by spectroscopic and molecular

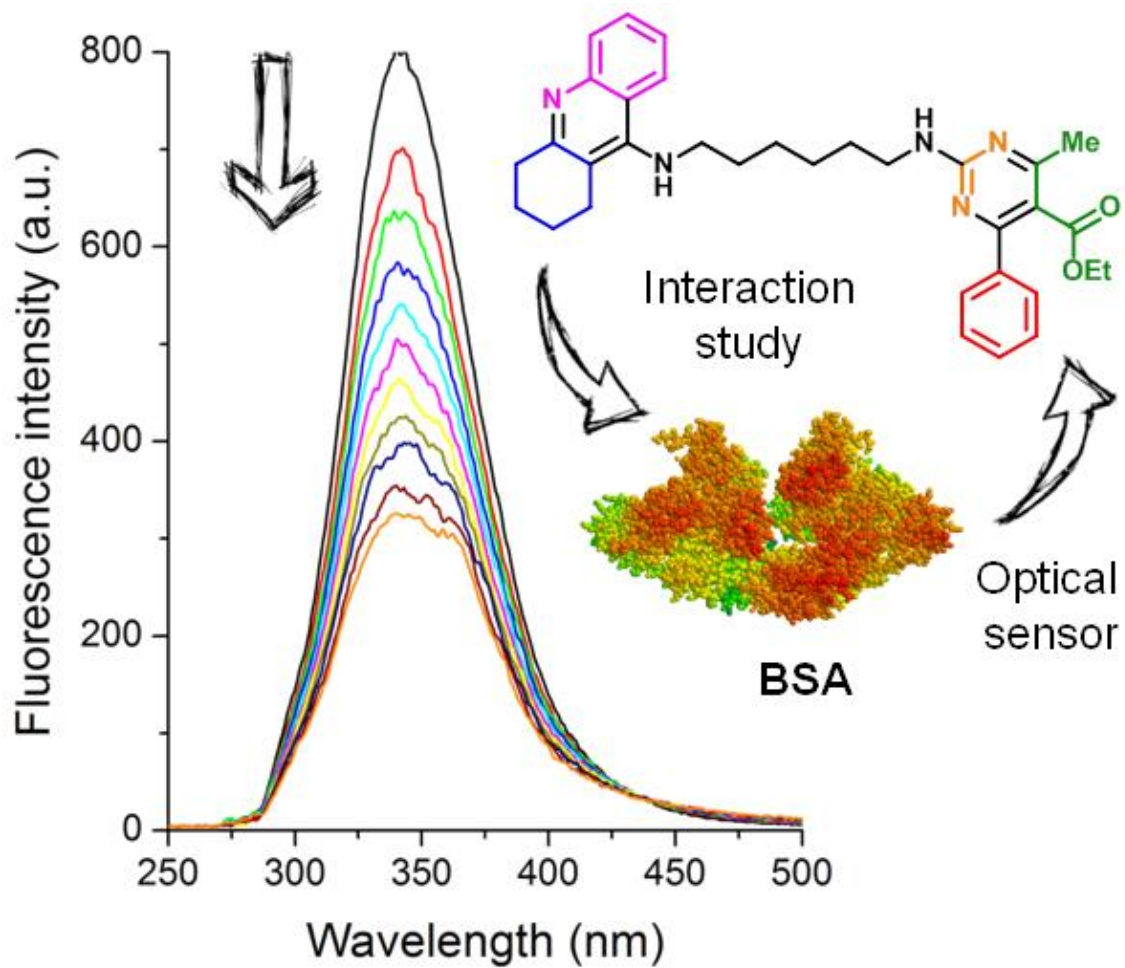
modeling techniques: a comparison study, *J. Biomol. Struct. Dyn.* 33 (2014) 513-533.

[57] F. Ramezani, H. Rafii-Tabar, An in-depth view of human serum albumin corona on gold nanoparticles, *Mol. Biosyst.* 2 (2015) 454-62.

[58] Q. Wang, C.R. Huang, M. Jiang, Y.Y. Zhu, J. Wang, J. Chen, J.H. Shi, Binding interaction of atorvastatin with bovine serum albumin: Spectroscopic methods and molecular docking, *Spectrochim. Acta A* 156 (2016) 155-163.

ACCEPTED MANUSCRIPT

Graphical Abstract



Highlights

- Molecular hybrids from Tacrine and pyrimidine achieved by multicomponent reaction
- Photoactive molecular hybrids in the violet region of the spectra (~400 nm)
- Bovine serum albumin (BSA) fluorescence suppression due to the pyrimidine moiety

ACCEPTED MANUSCRIPT